AGU ADVANCING EARTH AND SPACE SCIENCE

Earth and Space Science

RESEARCH ARTICLE
10.1029/2022EA002407

Key Points:

- The charge carried by precipitation particles is closely related to the microphysical processes in thunderstorms
- The bulk of the measured charged raindrops are the larger than 1 mm
- A correlation between the sizes and the charges carried by the raindrops was found, in good agreement with the non-inductive mechanism

Correspondence to:
E. Ávila,
eldoavila@gmail.com

Citation:
Ávila, E., Martínez, L., Pereyra, R., Lang, T., Deierling, W., Wingo, M., et al. (2022). Measurements of size and electrical charges carried by precipitation particles during RELAMPAGO field campaign. *Earth and Space Science*, *9*, e2022EA002407. https://doi.org/10.1029/2022EA002407

Received 1 MAY 2022
Accepted 3 SEP 2022

Author Contributions:

Conceptualization: Eldo Ávila, Rodolfo Pereyra, Timothy Lang, Matthew Wingo
Formal analysis: Eldo Ávila, Lucia Martínez, Rodolfo Pereyra, Timothy Lang, Wiebke Deierling, Gregory Melo, Bruno Medina
Investigation: Eldo Ávila, Lucia Martínez, Rodolfo Pereyra, Timothy Lang, Wiebke Deierling, Gregory Melo
Methodology: Eldo Ávila, Lucia Martínez, Rodolfo Pereyra, Timothy Lang, Wiebke Deierling, Matthew Wingo, Gregory Melo
Software: Lucia Martínez, Rodolfo Pereyra, Timothy Lang, Matthew Wingo
Supervision: Eldo Ávila

Measurements of Size and Electrical Charges Carried by Precipitation Particles During RELAMPAGO Field Campaign

Eldo Ávila[1], Lucia Martínez[1], Rodolfo Pereyra[1], Timothy Lang[2], Wiebke Deierling[3], Matthew Wingo[4], Gregory Melo[5], and Bruno Medina[3]

[1]Facultad de Matemática, Astronomía y Física, Universidad Nacional de Córdoba, IFEG-CONICET, Córdoba, Argentina, [2]NASA Marshall Space Flight Center, Huntsville, AL, USA, [3]University of Colorado Boulder, Boulder, CO, USA, [4]University of Alabama in Huntsville, Huntsville, AL, USA, [5]National Weather Service Office Indianapolis, Indianapolis, IN, USA

Abstract The electrical charge carried by raindrops provides significant information about thunderstorm electrification mechanisms, since the charge acquired by hydrometeors is closely related to the microphysical processes that they undergo within clouds. Investigation of charges on raindrops was conducted during the Remote sensing of Electrification, Lightning, And Meso-scale/micro-scale Processes with Adaptive Ground Observations field campaign. A newly designed instrument was used to determine simultaneously the fall velocity and charge for precipitating particles. Hydrometeor size and charge were measured in Córdoba city, Argentina, during electrified storms. Temporal series of size-charge of single raindrops were recorded for two storms, which were also monitored with a Parsivel disdrometer and Lightning Mapping Array. The results show that the magnitude of the electric charges range between 1 and 50 pC and more than 90% of the charges are mainly carried by raindrops >1 mm, even though most of the raindrops are smaller than 1 mm. Furthermore, the measurement series show charged hydrometeors of both signs all the time. A correlation between the sizes and the charges carried by the raindrops was found in both storms.

1. Introduction

Field observations suggest that the electrification of the thunderstorms is a consequence of the interactions between the dynamics and microphysics of clouds. There is observational and laboratory evidence that the non-inductive mechanism (NIM) is the mechanism responsible for the complicated electrical structures of thunderstorms. NIM is based on the collisions between ice particles (graupel/ice crystals, snowflakes/ice crystals, and large graupel/small graupel) and the selective charging of the larger particles with one sign. Then, the gravitational separation of the large and small particles can lead to the observed electrical structures of thunderstorms. Therefore, graupel particles play a key role in the thunderstorm electrification processes (See MacGorman & Rust, 1998 and references therein).

Laboratory studies show that graupel particles acquire electric charge as a result of collisions with ice crystals. The acquired charge depends on the thermodynamic and microphysical conditions of the environment, as well as the surface states of each of the interacting particles (Pereyra et al., 2000; Reynolds et al., 1957; Saunders et al., 1991, 1999, 2001; Takahashi, 1978).

The physical mechanism responsible for charge separation in ice crystal/graupel collisions is very complex. In laboratory studies of single ice crystal/graupel collisions, it has been observed that the charge sign of the graupel can generally be of either sign, with a predominance of one of them, depending on the environmental conditions and the surface state of the interacting particles (Ávila et al., 1996; Caranti et al., 1991; Gaskell & Illingworth, 1980; Pereyra & Avila, 2002). The electrical structure of thunderstorms is also extremely complex and variable, likely as a consequence of the complex charge separation mechanism and the complexity of the air mass movements within the storms.

Knowledge of the electric charge carried by raindrops can provide useful information about thunderstorm electrification mechanisms, since charging is closely linked to the microphysical processes that hydrometeors undergo within clouds.

Gunn (1949) observed the charge of raindrops on the ground below active thunderstorms in Washington, D.C., and found that the mean electric charge of raindrops had a magnitude of 4 pC. Despiau and Houngninou (1996) measured electric charges of raindrops on the ground and found that 90% of them carried a positive charge of

Validation: Lucia Martínez, Rodolfo Pereyra, Timothy Lang, Wiebke Deierling, Matthew Wingo
Writing – original draft: Eldo Ávila
Writing – review & editing: Timothy Lang, Wiebke Deierling

average value 86 pC, while the average negative charge was −22 pC. It is important to note that they detected drops having charges magnitude >3 pC.

In thunderstorms, Gunn (1947) measured the electrical charge on raindrops at various altitudes. They observed average positive charges of 10 pC between 3 and 8 km and negative charges of 13 pC up to 6 km. Takahashi (1965) by using a radiosonde, observed a charge of 16 pC on raindrops of about 3 mm in diameter.

More recent measurements of charge on hydrometeors have been made using aircraft and balloons (Bateman et al., 1999; Bringi et al., 1997; Dye et al., 1986; Gardiner et al., 1985). Airborne instruments combining optical imaging probe and induction rings have also been used (Christian et al., 1980; Gaskell et al., 1978; Mo et al., 2007; Weinheimer et al., 1991).

Mo et al. (2007) measured charged precipitation particles from an instrumented aircraft that passed through a tenuous precipitation. They found that 98% of the charged particles carried positive charge; 68% of the particles carried charge >0.5 pC and observed maximum charge of 25 pC. They also observed a trend for larger particles to carry larger charge magnitude.

Balloon observations of charge and size of precipitation particle provide information about vertical charge profiles in thunderstorms (Bateman et al., 1999). These studies show that key information about the fundamental electrical processes within thunderstorms can be obtained through detailed studies of the electrical charges carried by raindrops.

Although there is a series of published studies in the literature of the charge of precipitation particles and the microphysical characteristics of clouds, it is very important to continue with more quantitative and statistically robust studies. Knowing the kind of hydrometeors carrying electric charge in thunderstorms, and the relationship between their size and charge, it could be possible to discern whether NIM actually contributes to thunderstorm electrification, as well as having a better knowledge of the electrical structure of the storms.

In this work, we present ground observations of size and electric charges carried by precipitation particles. Temporal series of size-charge of single raindrops were recorded for two storms, which were in turn monitored with a Parsivel disdrometer and Lightning Mapping Array (LMA; Lang et al., 2020), during the field campaign called Remote sensing of Electrification, Lightning, And Meso-scale/micro-scale Processes with Adaptive Ground Observations (RELAMPAGO; Nesbitt et al., 2021).

2. Experimental Method

In order to determine the sign and magnitude of the charge of raindrops, as well as their diameter and fall speed, a specially designed experimental device was built in the Atmospheric Physics Group of the University of Córdoba, together with a set of software specially developed to obtain the desired parameters.

A photograph and a schematic of the device are shown in Figures 1a and 1b, respectively. The device is formed by seven bronze induction rings 10 cm in diameter, 5 cm high, and 1 mm thick. They are positioned on the external surface of a Teflon tube and separated by a distance of 2 mm, so that there is no electrical contact between them. Three of the rings are connected to inverting current-voltage amplifier circuits ("active" rings). The other four rings (passive rings) are connected to ground. The distance between the centers of two active rings is (10.6 ± 0.2) cm. The Teflon tube with the rings and the amplifier circuit are located inside an aluminum cylindrical structure. The amplifier is connected to an analog-digital converter, which was used connected to a computer with the necessary software to record the data. This instrument is capable of detecting electric charges >0.3 pC.

When an electrically charged raindrop passes through one of the active rings, it causes a current pulse due to the electric charge induced on it. The pulse is in the form of a descending and ascending wave, or ascending and descending, depending on the charge sign. This current is converted into voltage as it passes through the current-voltage amplifier and is recorded every 1 ms. The signal produced by the passage through each ring is recorded in different channels, as shown in Figure 2 with different colors representing the pulses generated in each active ring.

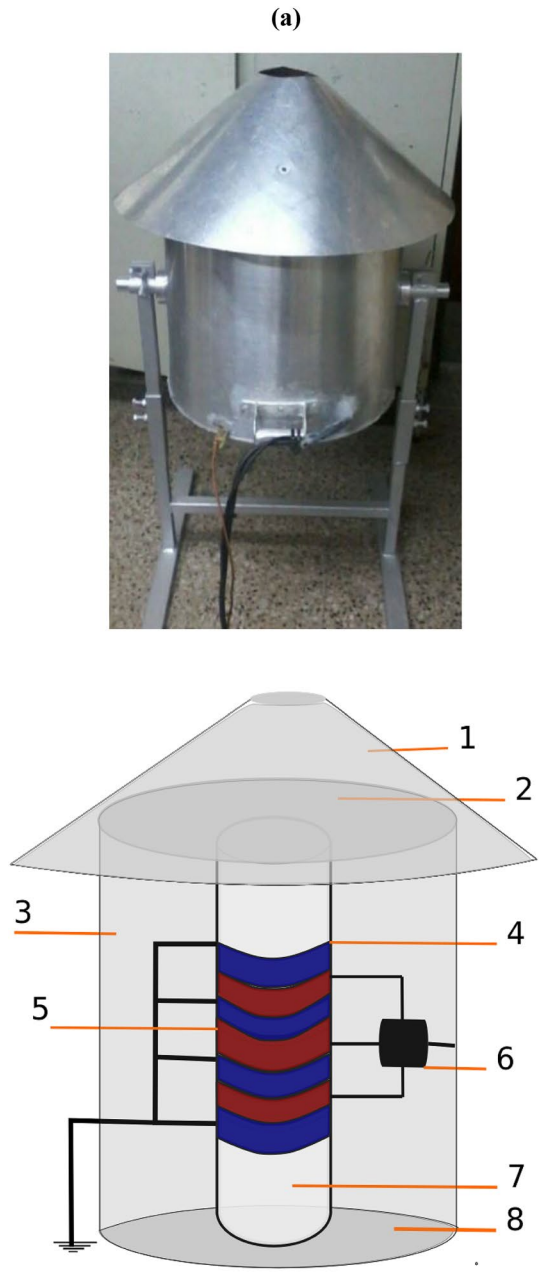

Figure 1. (a) Photograph and (b) a schematic of the experimental device. The device is formed by seven bronze induction rings 10 cm in diameter, 5 cm high, and 1 mm thick. Three of the rings (5) are connected to an inverting current-voltage amplifier circuit (6). The other four rings (4) are connected to ground. The Teflon tube (7) with the rings and the amplifier circuit are located inside an aluminum cylindrical structure (1, 2, 3, and 8).

The data obtained by each induction ring are used to obtain the electrical charge, by means of a time integration of the registered voltage, which is proportional to the current. The time integration is performed with software and the electric charge induced in each ring is obtained. The final charge (Q) is the average of the three charges and the uncertainty assigned to the average charge is the deviation from the average.

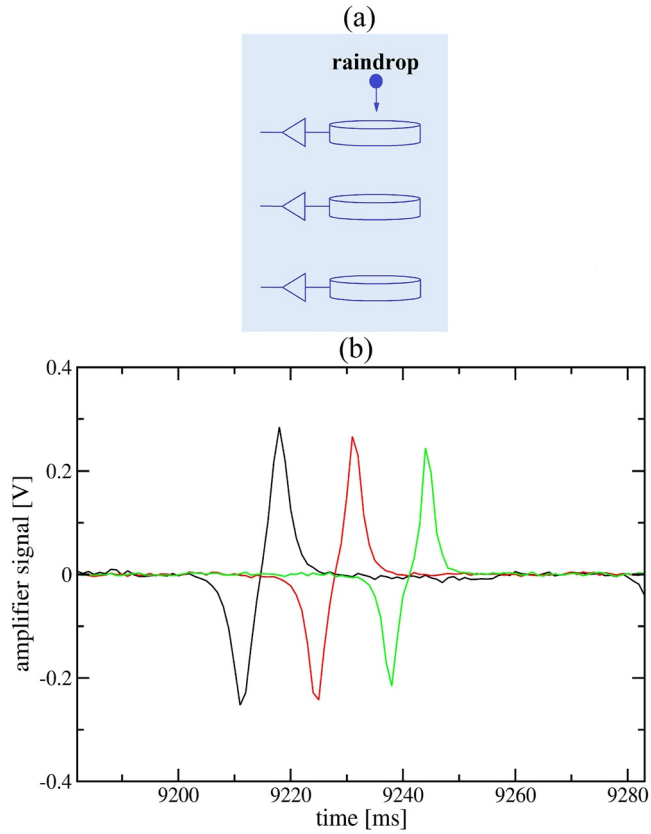

Figure 2. (a) An electrically charged raindrop passes through of the active rings connected to the amplifiers. (b) It produces three current pulses due to the electric charge induced on them. The pulse is in the form of a descending and ascending wave, or ascending and descending, depending on the charge sign. Different colors represent the pulses generated in each active ring.

This device used to determine the electrical charges carried by raindrops was checked and calibrated by measuring falling drops with previously known charges determined by means of a Keithley 610C Electrometer.

The vertical fall velocity of raindrops (V) is determined by measuring their time of passage between two induction rings. Assuming that the vertical fall speed is equal to the terminal fall speed; then the raindrop diameters can be obtained from the equations proposed by Beard (1976). In particular the V versus D parameterizations in the ranges 19 μm < D < 1 mm and 1 < D < 7 mm were used in this work.

The data provided by a Parsivel disdrometer fixed at a distance of 10 m from device to measure raindrops charge were also used in this study. The disdrometer is a laser-based instrument designed to measure and count simultaneously the fall velocity and size of precipitation particles (Tokay et al., 2014 and references within).

Between November 2018 and April 2019, an 11-station very high frequency (VHF) LMA was deployed to Córdoba Province, Argentina (Lang et al., 2020), coordinated with the RELAMPAGO field campaign (Nesbitt et al., 2021). The data provided by this field campaign were also used in the current work.

3. Measurements

The instrument built to measure the charge of raindrops and the disdrometer were located on the campus of the University of Córdoba on the roof of FAMAF building sited at (31° 26′ 17.48″S, 64° 11′ 36.76″W).

3.1. Storm on 20 December 2018

The rainfall at the ground occurred during 20:20–21:00 UTC as sensed by the disdrometer. Satellite images of the cloud-top temperature (CTT) corresponding at 10.33-μm channel, are shown in Figure 3a. The arrow

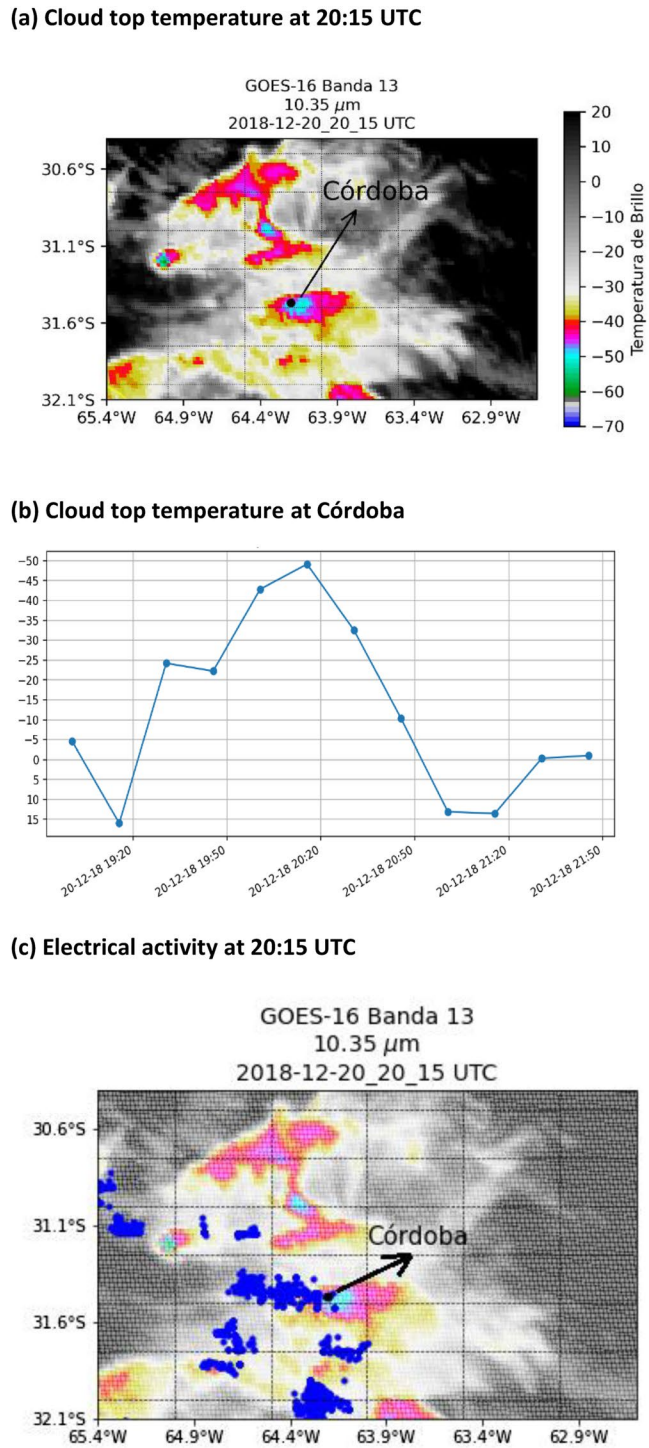

Figure 3. (a) Satellite images of the cloud-top temperature (CTT) at 20:15 UTC, corresponding to the storm on 20 December 2018. (b) Time evolution of the CTT over Córdoba city between 18:50 up to 21:50 UTC. (c) The electrical activity on the region corresponding at 20:15 UTC as detected by GOES. Satellite images and CTT evolution allows to observe that between 19:50 and 20:50 UTC a very localized thunderstorm with a minimum CTT around −50°C was developed over Córdoba city.

indicates where Córdoba city is located. This figure displays the storm situation at 20:15 UTC, the location of Córdoba city is indicated in the map. Figure 3b shows the time evolution of the CTT over Córdoba city between 18:50 and 21:50 UTC. Satellite images and CTT evolution showed that between 19:50 and 20:50 UTC a very localized thunderstorm with a minimum CTT around −50°C was developed over Córdoba city. Figure 3c

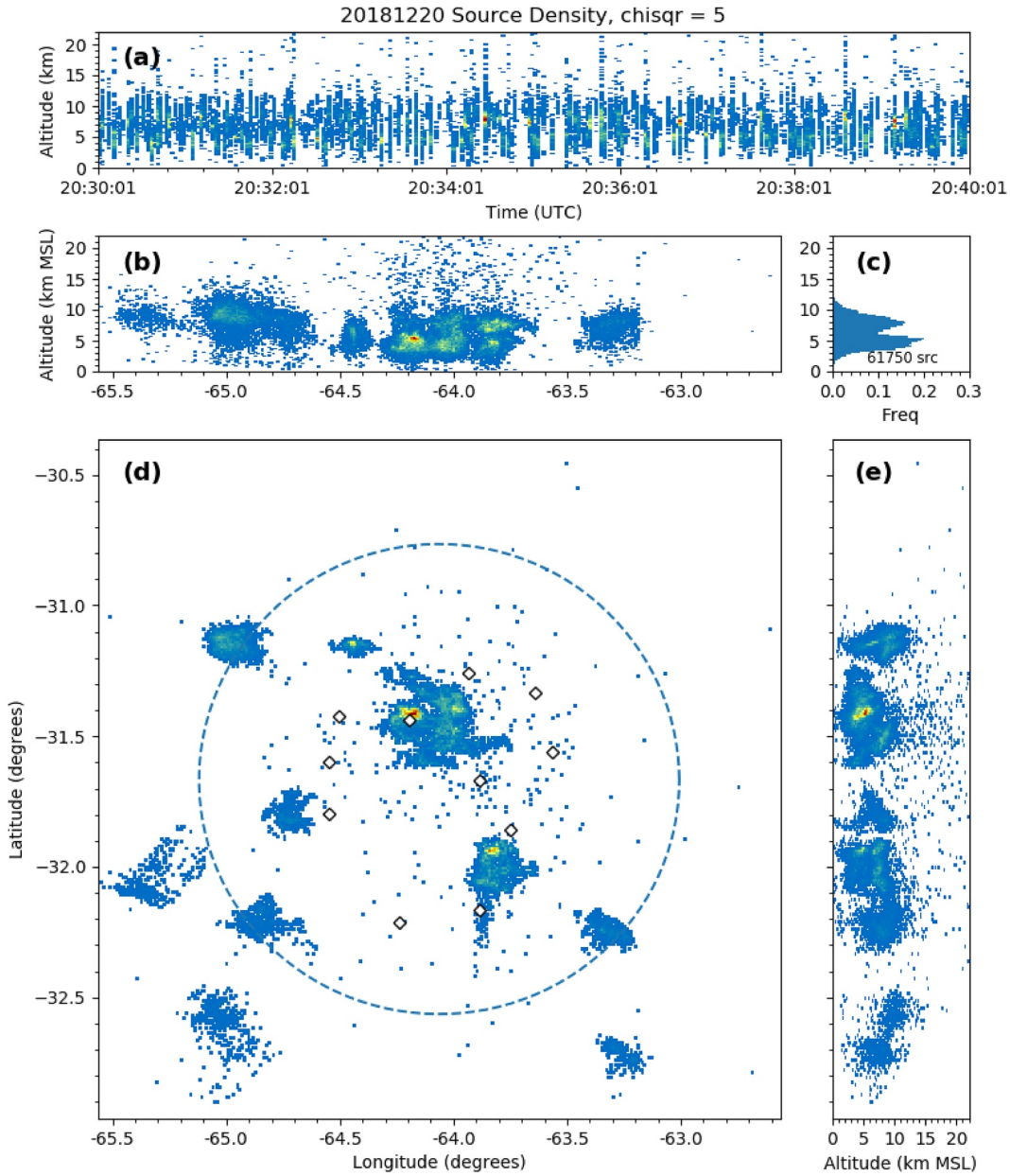

Figure 4. XLMA-style plot for Lightning Mapping Array (LMA) source density for 20:30–20:40 UTC on 20 December 2018. (a) Time-height. (b) Longitude-height. (c) Normalized vertical distribution of sources, with total number of sources observed. (d) Plan view. Also shown are LMA station locations (white diamonds) and the 100-km range ring. (e) Latitude-height. (c) In all subplots save, the density color scale is relative and unique to that particular subplot—blue is the lowest density of sources and red the highest.

shows the electrical activity on the region corresponding at 20:15 UTC as detected by GOES and particularly the figure displays lightning over Córdoba city at that time.

Figure 4 displays the LMA source density in the region for 20:30–20:40 UTC. The results display significant electrical activity over Córdoba city (the station location near −64.2° longitude and −31.4° latitude) during the sampled time period which is in agreement with GOES images. Note the predominance of low-altitude sources in the vicinity of Córdoba. Lang et al. (2020) identified this storm as having an anomalous charge structure (i.e., low/mid-level positive and upper-level negative) around this time.

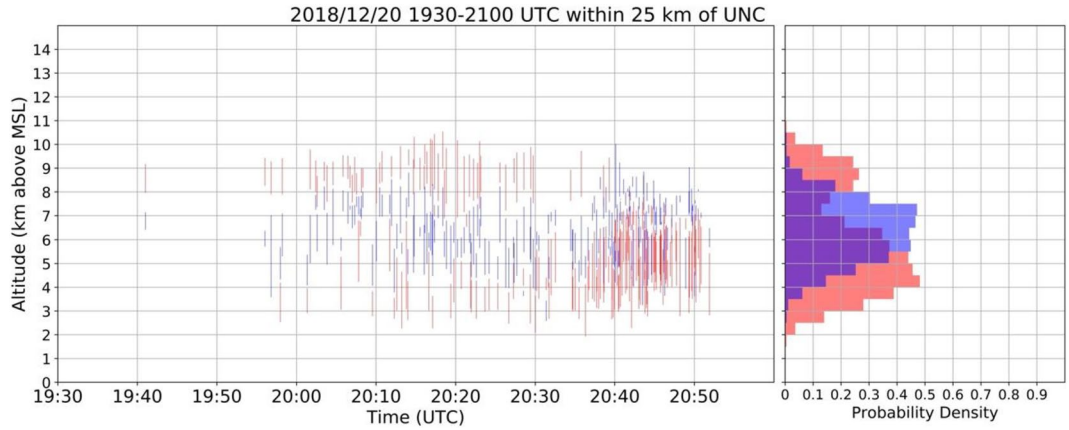

Figure 5. Left: Time-height plot of Chargepol-inferred charge layers (blue negative and red positive) associated with Lightning Mapping Array (LMA)-observed flashes within 25 km of the Córdoba LMA station location during 19:30–21:00 UTC on 20 December 2018. Right: Integrated vertical histogram over this time period of positive- and negative-inferred very high frequency sources (purple: positive and negative overlap).

The Chargepol analysis method was applied to the LMA observations from this case. As discussed by Medina et al. (2021), Chargepol automatically infers vertical charge distributions from LMA observations. For flashes containing at least 20 VHF sources, the vertical direction of the initial negative leader is determined. Charge layers are then identified by clustering the middle 80% of VHF sources above and below a threshold altitude (associated with the leader initiation) that separates the candidate sources for the two charge layers. Chargepol works on a representative minority of LMA-detected flashes, and Medina et al. (2021) demonstrated that—when applied for extended periods of time—it is capable of inferring a storm's bulk electrical charge structure and evolution during its life cycle. The Chargepol results for 20 December 2018 are shown in Figure 5. Prior to 20:30 UTC, the storm displayed a normal tripolar structure. However, after 20:30 UTC a deep layer of low-to-mid-level positive charge developed, and this was associated with an increase in electrical activity (i.e., flash rate), in close agreement with the CTT evolution shown by GOES results. As described by Medina et al. (2021), this behavior is associated with

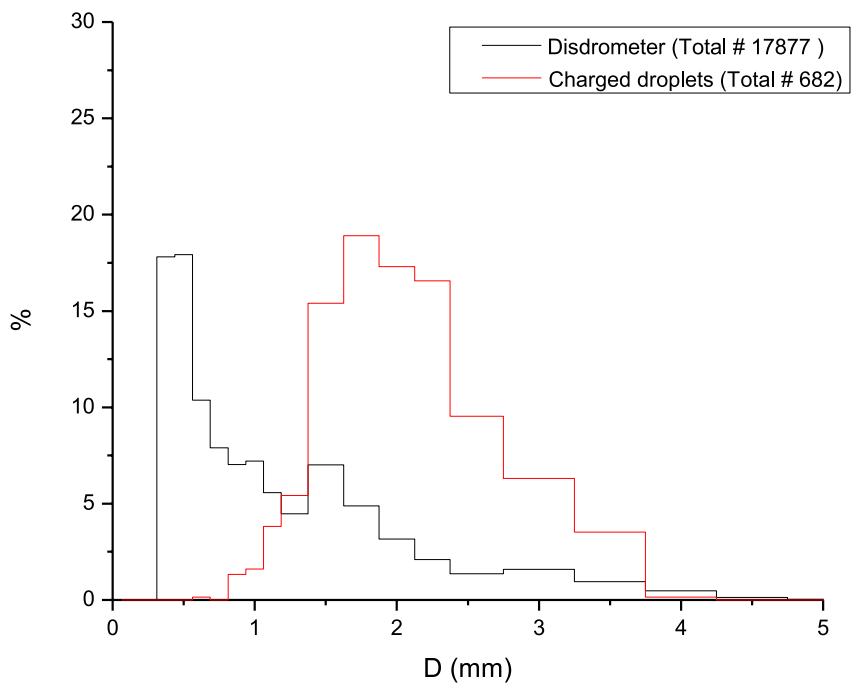

Figure 6. Size distribution of the raindrops corresponding to the storm on 20 December 2018 measured by the disdrometer (black line) and size distribution of the charged raindrops measured by the experimental device (red line).

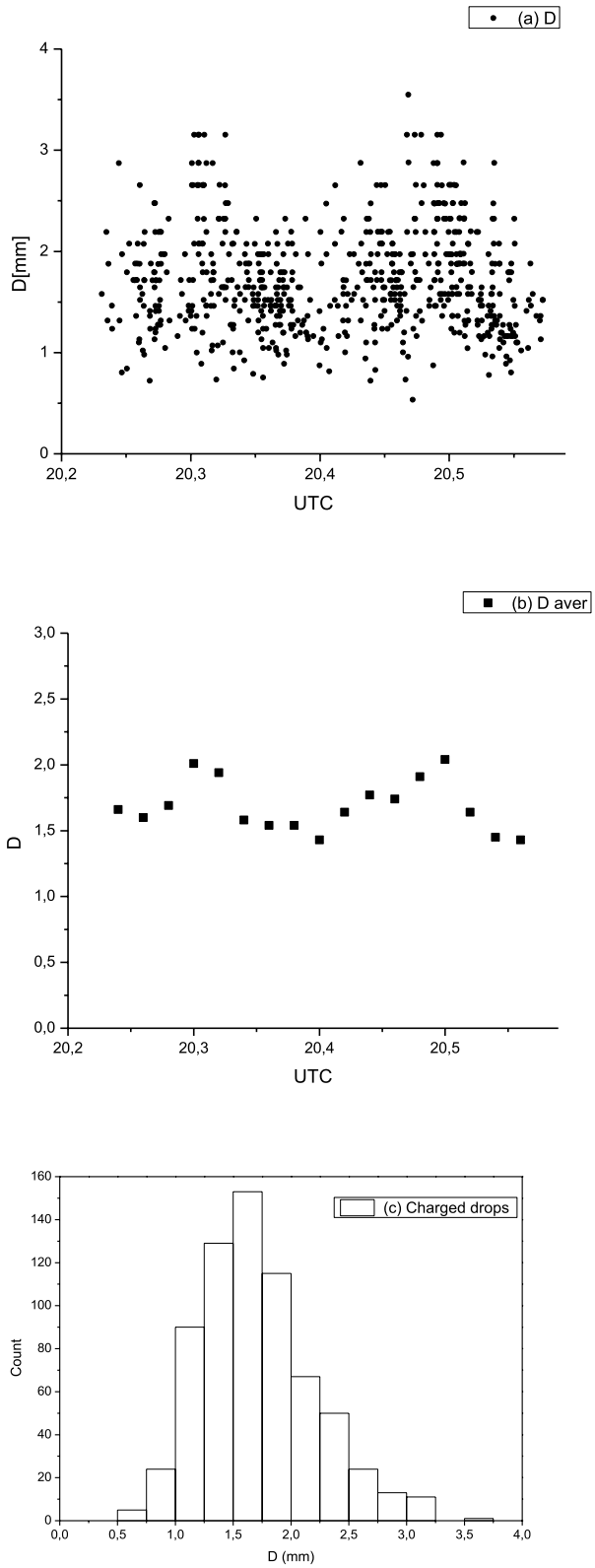

Figure 7. (a) Time evolution of the all charged raindrops (CR) diameter during the 20 December 2018 storm. (b) CR diameter averaged every 120 s. (c) The size distribution in 0.5 mm intervals of all the CR measured during the storm.

a storm developing an anomalous charge structure (i.e., mid-level positive charge under upper-level negative charge). Lang et al. (2020) also flagged this latter time period of the 20 December storm as consistent with an anomalous charge structure.

3.1.1. Charge and Size Measurements of Precipitation Particles

The measurement of charged raindrops (CR) started at 20:20 UTC and finished at 20:53 UTC, when charged particles stopped falling.

In order to compare the raindrop sizes (detected by the disdrometer) and CR sizes, the size histograms obtained with each instrument were contrasted. Figure 6 shows the drop size distribution measured by the disdrometer (black line) and CR size distribution (red line). The disdrometer measured a peak of the raindrop size around 0.5 mm, while the CR histogram has a maximum around 1.8 mm. It is observed that more than 70% of the raindrops measured by the disdrometer have sizes less than 1 mm, while more than 90% of the CR have sizes between 1 and 3 mm. It is important to remark that our instrument is able of detecting raindrops of 0.5 mm carrying electric charges as small as 0.3 pC; therefore, the scarcity of CR smaller than 1 mm suggests that preferentially the electric charge is carried by larger raindrops (>1 mm).

Figure 7a shows the time evolution of the CR diameters (D) from the beginning of the rain. Figure 7b shows the CR diameters averaged every 120 s. The average D remained fairly constant, varying between 1.5 and 2.0 mm. Figure 7c displays the size distribution of all the CR measured during the storm. The total number of CR recorded was 682, 4% of the CR were <1 mm, 82% of the CR were between 1 and 2 mm with the distribution peaking at 1.5 mm, and 14% of the CR were >2 mm.

The time evolution of the charge carried by the raindrops measured during the storm is shown in Figure 8a. Charges (Q) in the range [−30, 50] pC were recorded and most of drops carried charges in the range [−10, 20] pC. The main characteristic observed is that most of the charge magnitude $|Q| > 1$ pC and a mixed charge sign were registered all the time.

A predominance of positive charge at the beginning of the rain can be noted up to around 20:40 UTC (~during the first 1,000 s). This trend is reversed after 20:40 UTC and a predominance of negative charge is observed during the last part of the rainfall. This result is confirmed when the charge is averaged every 120 s as shown in Figure 8b. The results clearly show that there is a predominance of positive charge during the first part of the rain and then it reverses to negative up to the end of the rain. This is consistent with the observed anomalous charge structure in the storm (Figures 4 and 5)—predominantly positive charge would be expected early as this layer was closest to the ground. As time went on, however, predominantly negatively charged particles from the storm's upper levels would be expected to precipitate to the ground.

The possible correlation between the sizes and the charges carried by the raindrops was analyzed. For this, the positive and negative drops were analyzed separately. The drops were separated into 0.5-mm intervals and the average charge of the drops within each interval was assigned to them. Figure 9 displays the average charges as a function of the CR sizes. The results show a clear tendency for the magnitude of the charge to grow for larger CR. This behavior is similar for both positive and negative raindrops. The slope of the positive charges is (1.8 ± 0.3) pC/mm and for negatives charges is (1.2 ± 0.3) pC/mm.

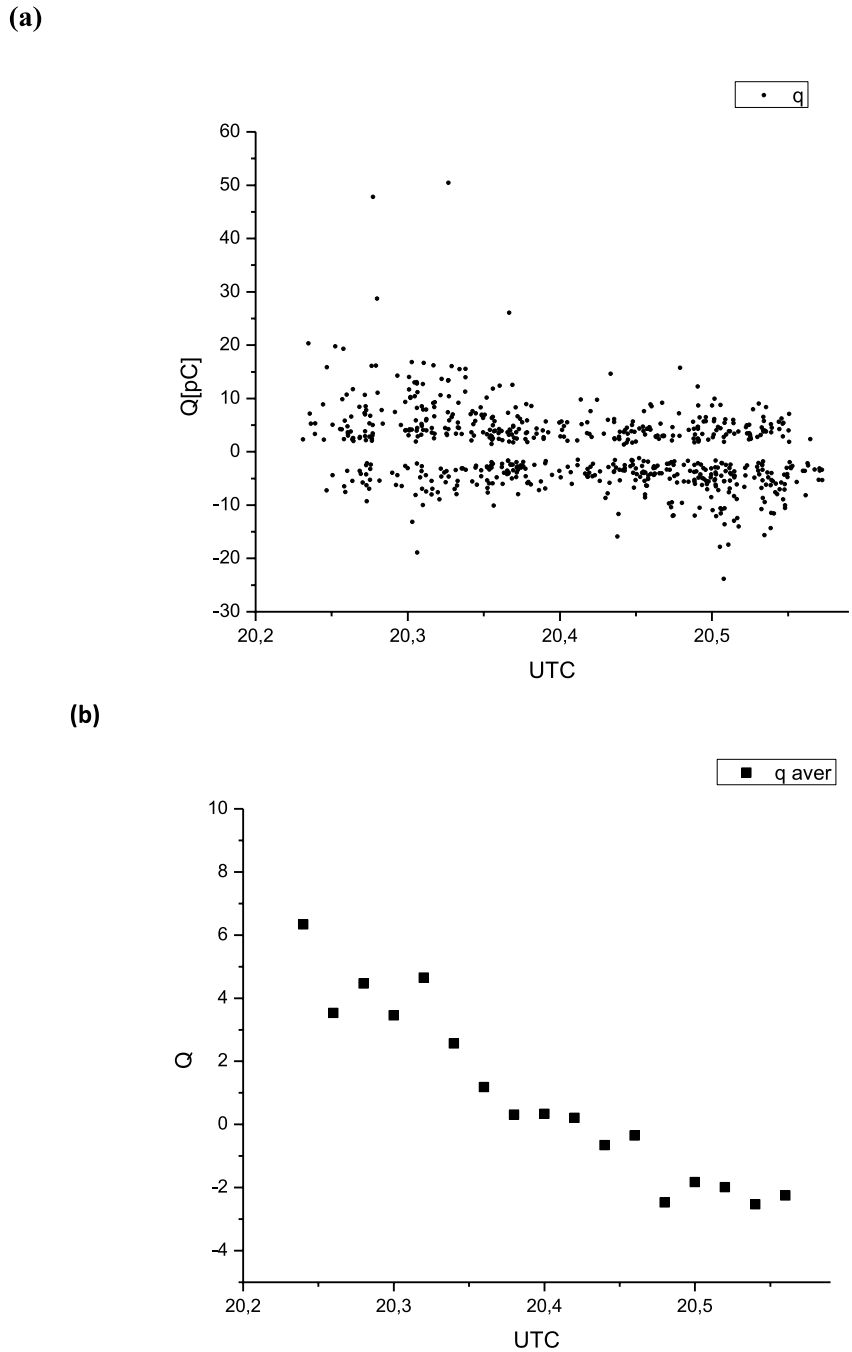

Figure 8. (a) Time evolution of the raindrop charges during the 20 December 2018 storm. (b) Raindrop charges averaged every 120 s. A predominance of positive charge during the first part of the rain and then it reverses to negative up to the end of the rain.

3.2. Storm on 17 March 2019

The rain occurred between 04:00 and 05:00 UTC. The measurement of charged precipitation particles started at 04:20 UTC and lasted for 30 min Figure 10a displays the satellite images of the CTT corresponding at 04:00 UTC. The arrow indicates where Córdoba city is located. Figure 10b shows the time evolution of the CTT over Córdoba city from 03:20 to 05:50 UTC. The images show that between 03:00 and 04:40 UTC the CTT was between −44 and −36°C. GLM measured lightning over Córdoba between 04:00 and 04:30 UTC. Figure 10c shows the lightning activity on the region corresponding at 04:15 UTC. The figure displays lightning over Córdoba city at that time.

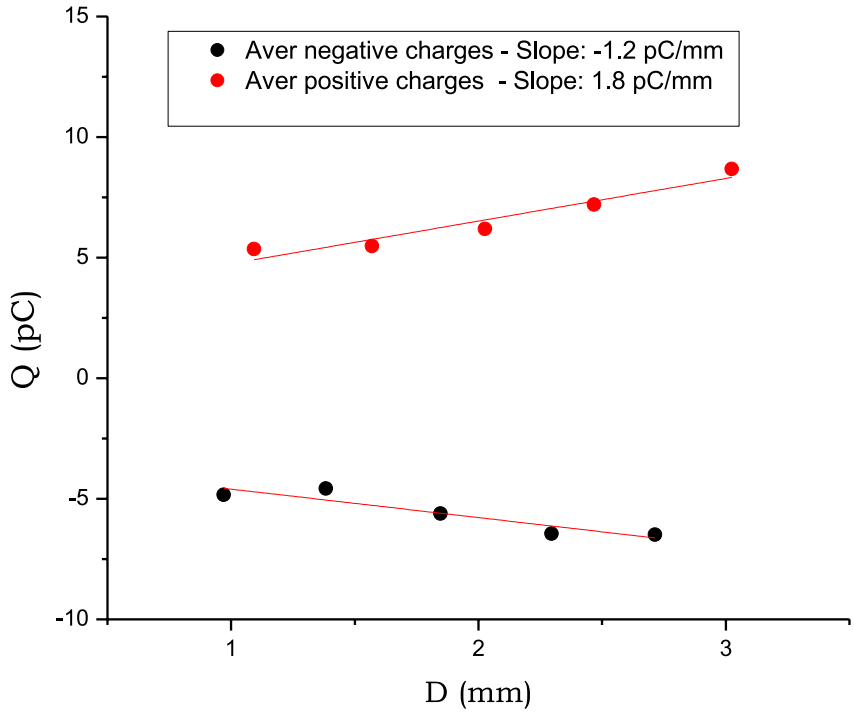

Figure 9. Correlation between the sizes and the charges carried by the raindrops. The positive (red) and negative (black) drops were analyzed separately. The slope of the positive charges is (1.8 ± 0.3) pC/mm and for negatives charges is (1.2 ± 0.3) pC/mm. A trend for the magnitude of the charge to grow for larger raindrops is observed.

Figure 11 displays the LMA source density in the region for 03:50–04:00 UTC. The results display some electrical activity over Córdoba city (the station location near −64.2° longitude and −31.4° latitude) during the sampled time period, which is in agreement with GOES images. Note again the predominance of low-altitude sources in the vicinity of Córdoba. However, unlike 20 December 2018, this resulted from the gradual descent and horizontal stratification of a decaying normal-polarity storm.

Figure 12 shows the Chargepol analysis for this storm during 02:30–05:00 UTC. The 100-km threshold was used instead of 25 km due to the weaker electrical activity in the general vicinity. However, as Figure 11 shows the altitude of the activity near Córdoba is similar to the altitudes of electrical activity elsewhere in the region. The results display moderate electrical activity over Córdoba region between 04:00 and 04:30 UTC and scarce activity after 04:30 UTC. Prior to 04:00 UTC, a gradual descent in lightning activity is observed as flash rate also decreases. This behavior is shown by Chargepol to indicate a decaying, normal-polarity tripole. However, many flashes after 03:45 UTC only involve the lowest two charge layers in the tripole.

3.2.1. Charge and Size Measurements of Precipitation Particles

The measurement of charged precipitation particles started at 04:20 UTC and finished at 04:50 UTC.

Figure 13 shows the drop size distribution measured by the disdrometer (black line) and CR size distribution (red line). The disdrometer measured a wide peak of the raindrop size between 0.3 and 0.9 mm, while the CR histogram has a maximum between 1.6 and 1.9 mm. It is observed that more than 60% of the raindrops measured by the disdrometer have sizes less than 1 mm, while more than 90% of the CR have sizes between 1 and 3 mm. Similarly to the previous storm, the scarcity of CR smaller than 1 mm suggests that preferentially the electric charge is carried by larger raindrops (>1 mm).

Figure 14a shows the evolution of the CR sizes during the rain. Figure 14b shows the CR diameter averaged every 120 s, the average size ranged between 1.3 and 1.7 mm. Figure 14c displays the size distribution of all the CR measured. The total number of CR recorded was 912; of which, 8% of the CR were <1 mm, 73% of the CR were between 1 and 2 mm with peak in 1.5 mm and 19% of the CR were >2 mm.

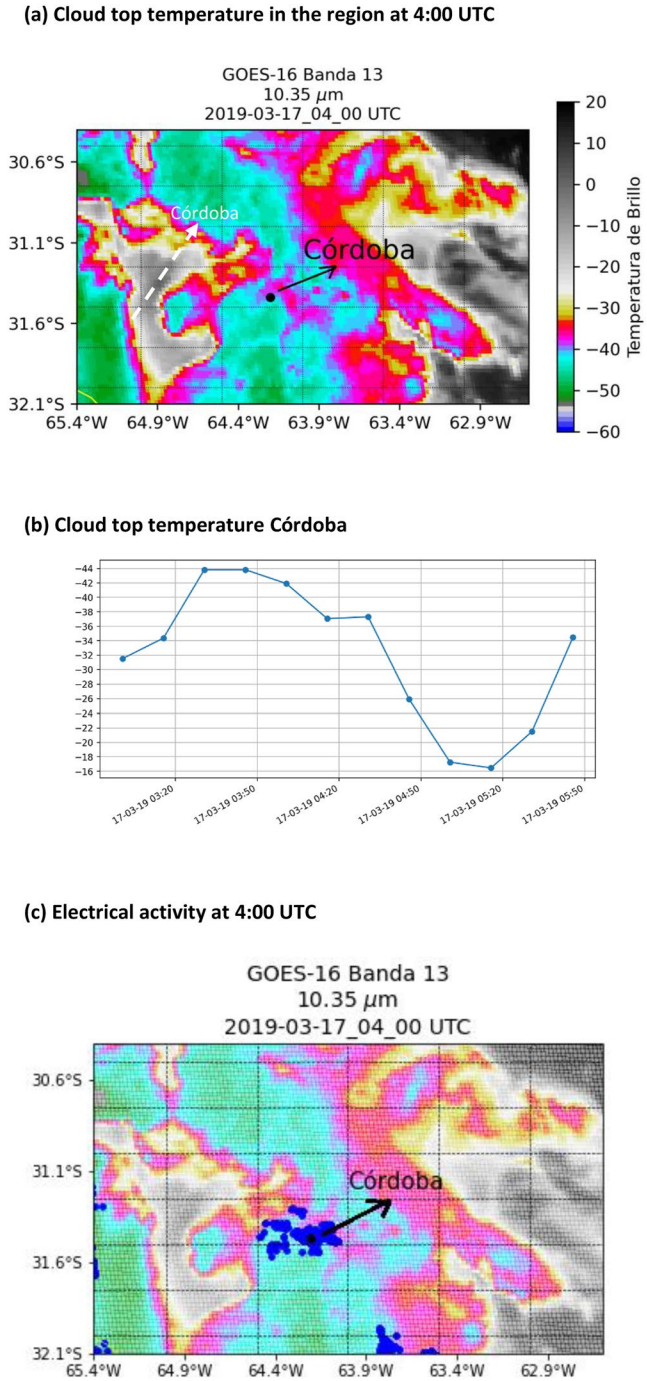

Figure 10. (a) Satellite images of the cloud-top temperature (CTT) at 4:00 UTC, corresponding to the storm on 17 March 2019. (b) Time evolution of the CTT over Córdoba city between 03:20 and 05:50 UTC. (c) The electrical activity on the region corresponding at 04:00 UTC as detected by GOES.

The time evolution of the sign and magnitude of the CR measured during the storm is shown in Figure 15a. Charges in the range [−20, 40] pC were recorded for this storm and most of CR carried charges in the range [−10, 10] pC. As in the previous storm most of the charges carried $|Q| > 1$ pC and a mixed charge sign were registered all the time. The averaged charge, in periods of 120 s, is displayed in Figure 15b. A predominance of negative charge at the beginning of the rain can be noted, this trend is reversed after 04:10 UTC (∼700 s after rain beginning) and a predominance of positive charge is observed. This behavior is the opposite of the previous

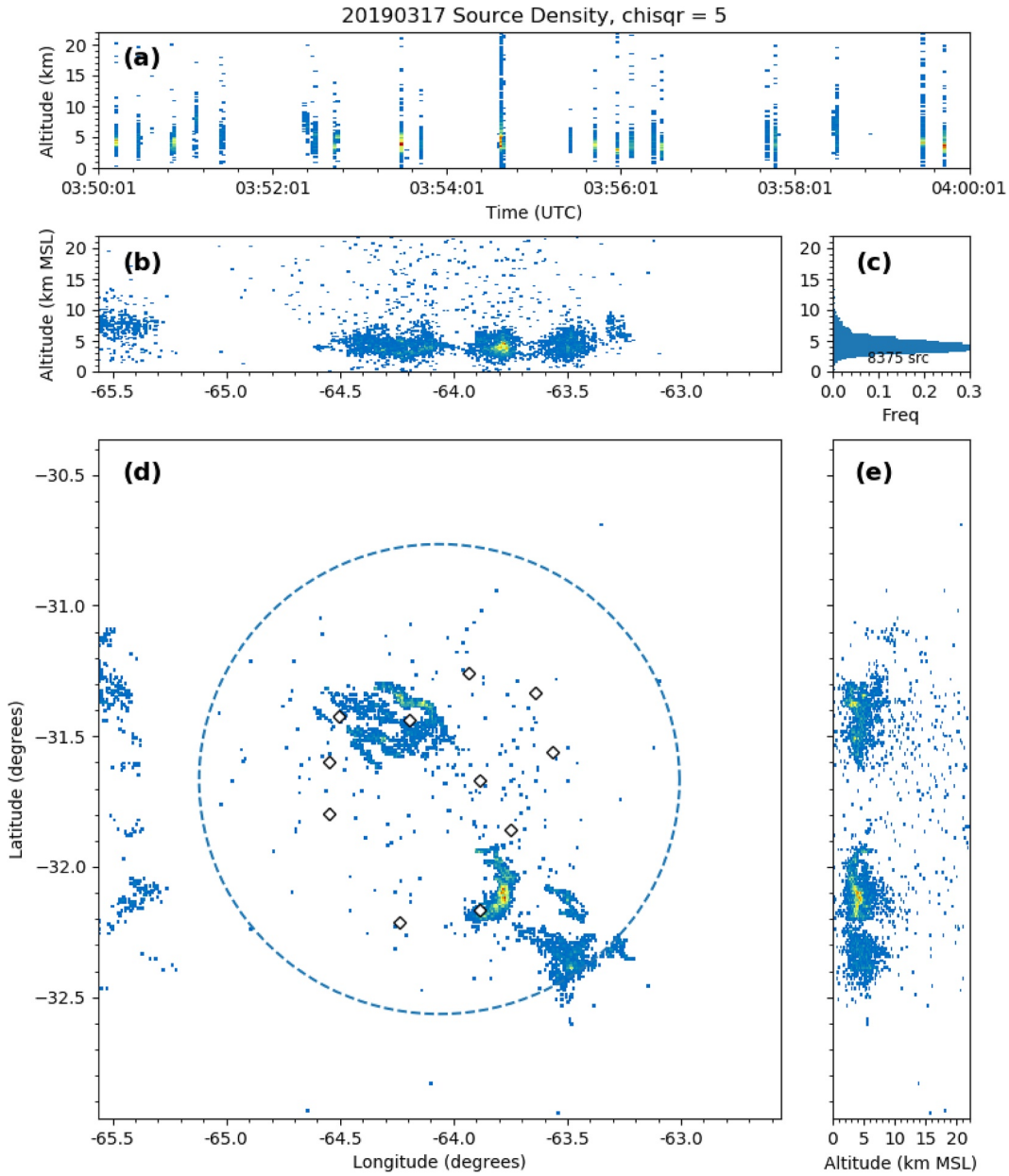

Figure 11. XLMA-style plot for Lightning Mapping Array (LMA) source density for 03:50–04:00 UTC on 17 March 2019. (a) Time-height. (b) Longitude-height. (c) Normalized vertical distribution of sources, with total number of sources observed. (d) Plan view. Also shown are LMA station locations (white diamonds) and the 100-km range ring. (e) Latitude-height. (c) In all subplots save, the density color scale is relative and unique to that particular subplot—blue is the lowest density of sources and red the highest.

storm. This is consistent with the LMA-inferred normal polarity of this decaying thunderstorm, where predominantly negative charge was closer to the ground than the positive charge (Figure 12). Thus, predominantly negatively charged particles ought to reach the ground before predominantly positive charged particles.

The correlation between the sizes and the charges carried by the raindrops was also analyzed for this storm. The drops were separated into 0.5 mm intervals and the average charge of the drops within each interval was assigned to them. Figure 16a and 16b displays the average charges as a function of the CR sizes. The results show a tendency for the magnitude of the charge to grow for larger CR. The slope of the positive charges is (1.6 ± 0.6) pC/mm and for negatives charges is (1.8 ± 0.1) pC/mm. This behavior is similar for both positive and negative raindrops. This behavior is consistent with the results of previous storm.

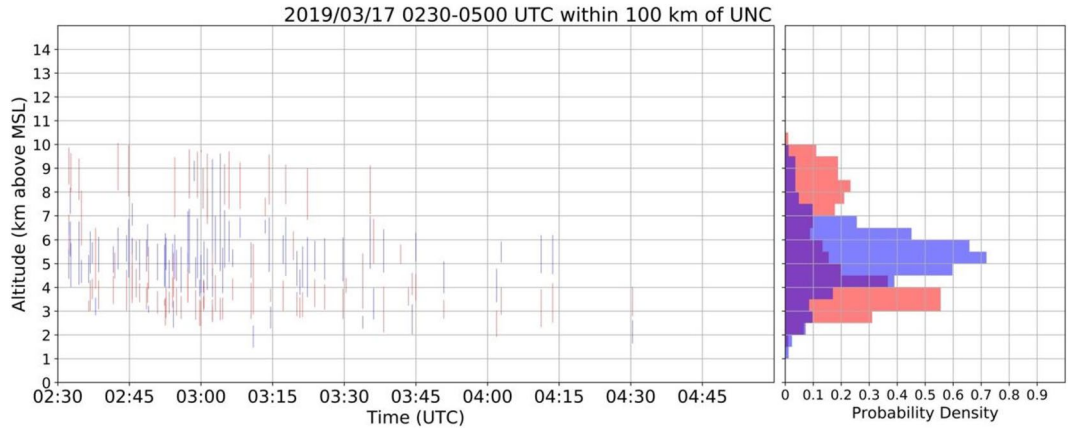

Figure 12. Left: Time-height plot of Chargepol-inferred charge layers (blue negative and red positive) associated with Lightning Mapping Array (LMA)-observed flashes within 10 km of the Córdoba LMA station location during 19:30–21:00 UTC on 17 March 2019. Right: Integrated vertical histogram over this time period of positive- and negative-inferred very high frequency sources (purple: positive and negative overlap).

4. Discussions

Both thunderstorms produced lightning activity registered by GOES and LMA network and reached minimum CTT < −40°C.

Regarding the characteristics of the storms, they presented several similarities, such as:

- Most of raindrops <1 mm.
- The variability range of the drop sizes is the same during the storm.
- Charge magnitudes $|Q| > 1$ pC were mainly detected.
- Mixed charge sign all the time.

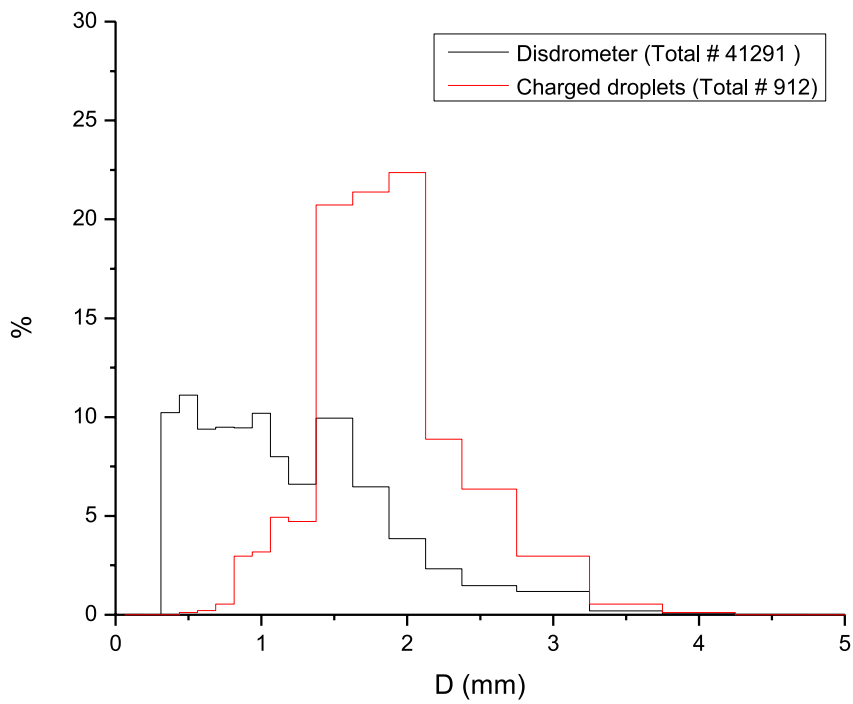

Figure 13. Size distribution of the raindrops corresponding to the storm on 17 March 2019 measured by the disdrometer (black line) and size distribution of the charged raindrops measured by the experimental device (red line).

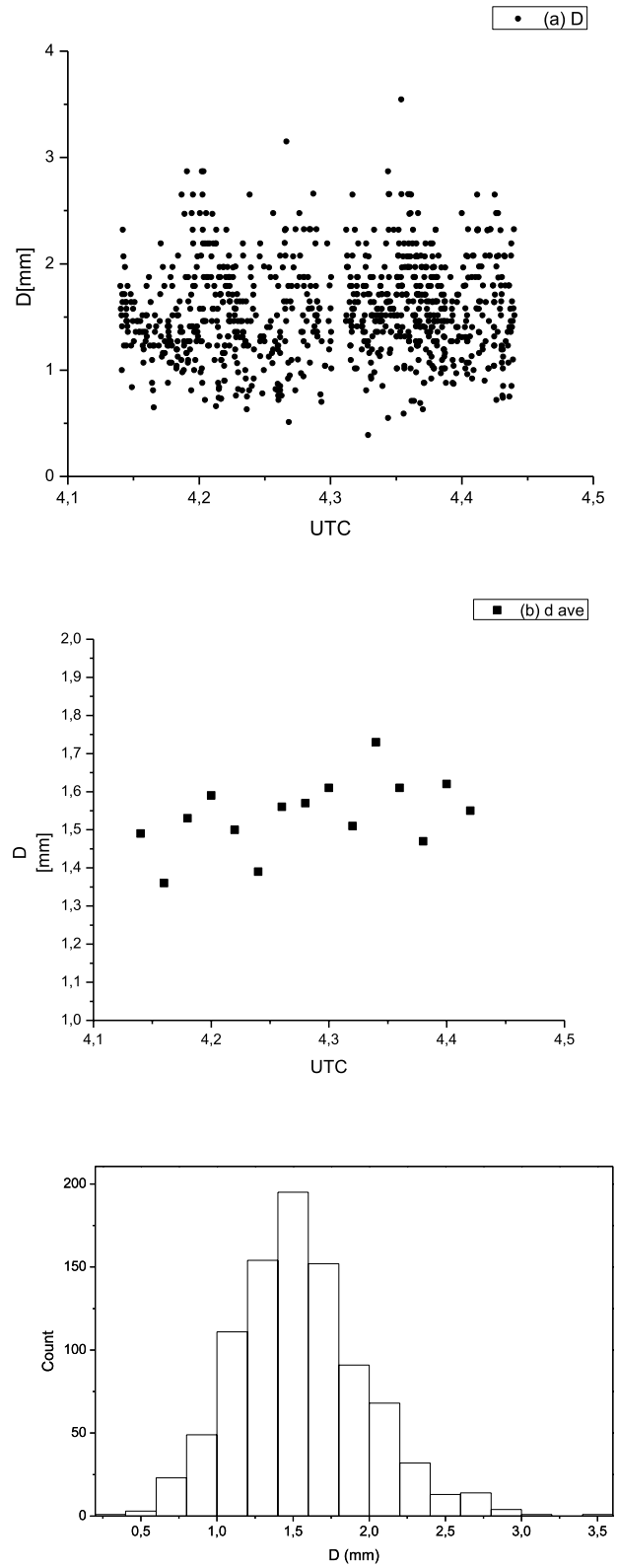

Figure 14. (a) Time evolution of the all charged raindrops (CR) diameter during the 17 March 2019 storm. (b) CR diameter averaged every 120 s. (c) The size distribution of all the CR measured during the storm.

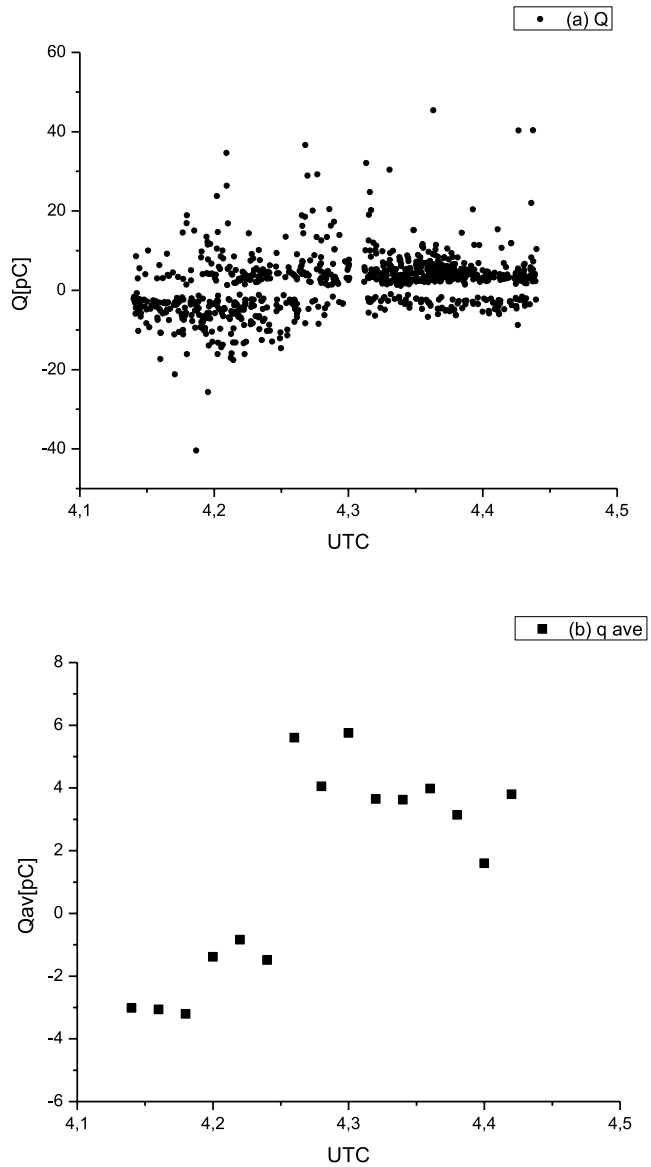

Figure 15. (a) Time evolution of the raindrop charges during the 17 March 2019 storm. (b) Raindrop charges averaged every 120 s. A predominance of negative charge during the first part of the rain and then it reverses to positive up to the end of the rain.

- Most of CR have sizes in the range 1–3 mm.
- A correlation between the sizes and the charges carried by the raindrops was found for both storms.

The literature reports conflicting data on the electric sign of raindrops. Some measurements found that negative droplets are predominant (Colgate & Romero, 1970; Magono & Kikuchi, 1961; Webb & Gunn, 1955). Other studies reveal that positively CR are predominant (Despiau & Houngninou, 1996; Gunn, 1952; Twomey, 1956). According to others (Phillips & Kinzer, 1958), including the current work, the number of negatively charged droplets is approximately equal to the number of positively charged droplets. Takahashi (1972) showed that the predominant electric sign changes with the sampling position in the storm. It is important to remark that varying conditions during different observations certainly could produce that many of the data appear contradictory or at least inconsistent with each other. For instance, chaotic air motions in storms could produce that two raindrops arriving one after the other at the observing instrument could have reached the ground after much different paths through the storm and experienced different growth histories. This also leads to the expectation of mixed polarity drops collected at a fixed site on the ground.

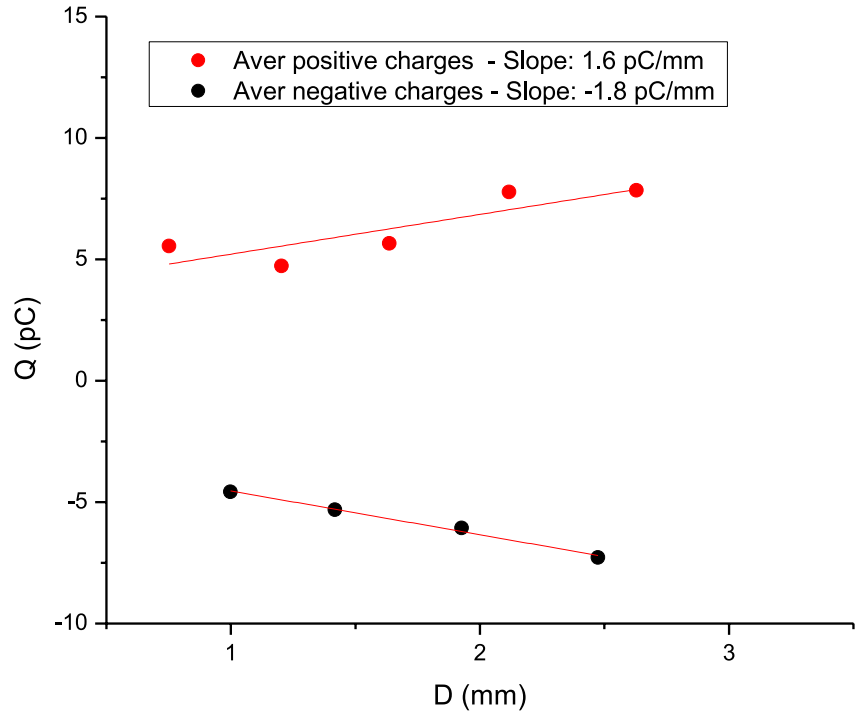

Figure 16. Correlation between the sizes and the charges carried by the raindrops. The positive (red) and negative (black) drops were analyzed separately. The slope of the positive charges is (1.6 ± 0.6) pC/mm and for negatives charges is (1.8 ± 0.1) pC/mm.

In principle, the present results are consistent with the NIM since the mechanism involves charge separation in collisions between ice crystals and graupel particles. In terms of the NIM graupel in the order of mm size accumulate charge through the impacts. During their fall and after crossing the 0°C isotherm, the graupel particles melt and turns into raindrops.

Raindrops of 1, 2, and 3 mm could have been spherical graupel of 2, 4, and 6 mm, respectively; this estimation was performed by taking an ice density of 0.2 g cm^{-3} which is quite reasonable for these graupel sizes (Macklin, 1962). This would then explain why raindrops carrying electric charges are the largest ones.

The correlations between the sizes and the charges (positives and negatives) carried by the raindrops are also consistent with the NIM since larger particles are expected to have a higher collision frequency of with ice crystals and therefore, they should become more charged. The analyzed storms show that, in average, the magnitude of the charge carried by the raindrops increases with a rate between 1 and 2 pC/mm, for both positive and negative CR.

On the other hand, the results found in this work appear inconsistent with the Inductive Mechanism (IM) of charge separation in thunderstorm, (Aufdermaur & Johnson, 1972; Scott & Levin, 1970). The IM proposes that in collisions between ice particles polarized in presence of an external electric field ($\boldsymbol{E}$), charge is transferred and the charged particles separate under gravity in a direction that increases the existing field. Then, the local $\boldsymbol{E}$ direction determines the sign that the large ice particles (graupel, hail, etc.) can acquire. The IM predict a maximum charge (Qm) that can be acquired by a precipitation particle in function of the diameter (d) and the vertical $\boldsymbol{E}$; it is (Sartor, 1967)

$$\mathrm{Qm} = 5.5\,|\boldsymbol{E}|\,d^2 \tag{1}$$

where d is given in mm, $|\boldsymbol{E}|$ in kV/cm and Qm in pC.

Considering the breakdown field of 3 kV/cm, the maximum charge allowed for the IM for 1 mm raindrops is 15 pC. The current results show that many of the CR of 1 mm carried a charge magnitude larger than those predicted by the IM. Thus the present measurements suggest that it does not seem possible that the IM played an important role in the studied storms.

It is important to note that when the raindrops fall to ground beneath thunderstorms, they cross a region with space charge due the presence of small ions. It is plausible to suppose that the space charge could modify the charge carried by the raindrops. Particularly, it is expectable to assume that the original charge be reduced due the neutralization of part of their charge. The question is how much the original charge can be reduced. Evidently, the charges are not completely neutralized due to it is possible to monitor their charge when they land on the ground.

On the one hand, it would be expected that the ion concentration decreases on time, due to raindrop scavenging. However, the results of the experiments do not show a substantial variation of the charge magnitudes. On the other hand, these charges are of the same order of magnitude as the charges measured within the storms. These arguments suggest that although there could be a reduction in the charge magnitude of the raindrops, this reduction would not be substantial enough to veil the charge that the drops have when they leave the cloud.

Regarding main differences between the both thunderstorms, we can highlight that the temporal evolution of the average charge of raindrops were different:

- In the 20 December 2018 storm the average CD was positive in the early part of the storm and then reversed to negative.
- In the 17 March 2019 storm the average CD was negative in the early part of the storm and then reversed to positive.

Clearly the falling sequence of the charged drops is directly related to the vertical electrical structure of the storm at the sampling site. The results of this work suggest that the vertical profiles of the electric charge distribution were completely different between the two measured storms. In particular, the ground-based observations provide useful validation of LMA-based inferences of thunderstorm charge structure.

Undoubtedly, considering the microphysical and dynamic properties of storms all together, it might be possible to make more detailed studies of the vertical electrical structure of storms and the possible evolution of them.

5. Summary and Conclusion

We presented a new series of measurements in which the size and electrical charges carried by precipitation particles were determined for two storms, which were in turn monitored with a Parsivel disdrometer and LMA network during the RELAMPAGO field campaigns.

An experimental setup was specially designed and constructed to determine simultaneously the fall velocity and charge for precipitating particles.

The analysis of the results has shown that most of the raindrops are smaller than 1 mm; while the charged hydrometeors are predominantly larger than 1 mm. The measurements show charged hydrometeors of both signs all the time and the charge magnitudes larger than 1 pC were mainly detected.

A correlation between the sizes and the charges carried by the raindrops was found in both storms. This result is consistent with the NIM since larger particles are expected to have a higher collision frequency of with ice crystals and therefore, they should become more charged.

It is emphasized that the knowledge of the electrical charge carried by raindrops can be of great relevance to obtain information about thunderstorm electrification mechanisms, since it is closely related to the microphysical processes that hydrometeors undergo within clouds. Furthermore, the temporal sequence of the CR can be of great relevance to obtain information about the vertical electrical structure of the storm at the sampling site.

Data Availability Statement

Lightning Mapping Array data are available from NASA (Lang, 2020, https://doi.org/10.5067/RELAMPAGO/LMA/DATA101). The raw data used to generate Figures 6–9 and 13–16 are available from FAMAF-UNC (https://www.famaf.unc.edu.ar/~pereyra/AGUSupporting-Information.pdf).

Acknowledgments
We thank Secretaría de Ciencia y Tecnología de la Universidad Nacional de Córdoba (UNC), Consejo Nacional de Investigaciones Científicas y Tecnológicas (CONICET), and Agencia Nacional de Promoción Científica (PICT 2019-2999) for their support.

References

Ávila, E. E., Varela, G. G. A., & Caranti, G. M. (1996). Charging in ice-ice collisions as a function of the ambient temperature and the larger particle average temperature. *Journal of Geophysical Research*, *101*(D23), 29609–29614. https://doi.org/10.1029/96jd01614

Aufdermaur, A. N., & Johnson, D. (1972). Charge separation due to riming in an electric field. *Quarterly Journal of the Royal Meteorological Society*, *98*(416), 369–382. https://doi.org/10.1002/qj.49709841609

Bateman, M. G., Marshall, T. C., Stolzenburg, M., & Rust, W. D. (1999). Precipitation charge and size measurements inside a New Mexico mountain thunderstorm. *Journal of Geophysical Research,* 104(D8), 9643–9653. https://doi.org/10.1029/1998jd200118

Beard, K. V. (1976). Terminal velocity and shape of cloud and precipitation drops aloft. *Journal of the Atmospheric Sciences*, *33*(5), 851–864. https://doi.org/10.1175/1520-0469(1976)033<0851:TVASOC>2.0.CO;2

Bringi, V. N., Knupp, K., Detwiler, A., Liu, L., Caylor, I. J., & Black, R. A. (1997). Evolution of a Florida thunderstorm during the convection and precipitation/electrification experiment: The case of 9 August 1991. *Monthly Weather Review*, *125*, 2131–2160. https://doi.org/10.1175/1520-0493(1997)125<2131:eoaftd>2.0.co;2

Caranti, J. M., Avila, E. E., & Re, M. A. (1991). Charge transfer during individual collisions in ice growing from vapor deposition. *Journal of Geophysical Research*, *96*(D8), 15365–15375. https://doi.org/10.1029/90jd02691

Christian, H., Holmes, C. R., Bullock, J. W., Gaskell, W., Illingworth, A. J., & Latham, J. (1980). Airborne and ground-based studies of thunderstorms in the vicinity of Langmuir Laboratory. *Quarterly Journal of the Royal Meteorological Society*, *106*(447), 159–174. https://doi.org/10.1002/qj.49710644711

Colgate, S. A., & Romero, J. M. (1970). Charge versus drop size in an electrified cloud. *Journal of Geophysical Research*, *75*(30), 5873–5881. https://doi.org/10.1029/jc075i030p05873

Despiau, S., & Houngninou, E. (1996). Raindrop charge, precipitation and Maxwell currents under tropical storms and showers. *Journal of Geophysical Research*, *101*(D10), 14991–14997. https://doi.org/10.1029/95jd03657

Dye, J. E., Jones, J. J., Winn, W. P., Cerni, T. A., Gardiner, B., Lamb, D., et al. (1986). Early electrification and precipitation development in a small, isolated Montana cumulonimbus. *Journal of Geophysical Research*, *91*(D1), 1231–1247. https://doi.org/10.1029/jd091id01p01231

Gardiner, B., Lamb, D., Pitter, R. L., Hallett, J., & Saunders, C. P. R. (1985). Measurements of initial potential gradient and particle charges in a Montana thunderstorm. *Journal of Geophysical Research*, *90*(D4), 6079–6086. https://doi.org/10.1029/jd090id04p06079

Gaskell, W., & Illingworth, A. J. (1980). Charge transfer accompanying individual collisions between ice particles and its role in thunderstorm electrification. *Quarterly Journal of the Royal Meteorological Society*, *106*(450), 841–854. https://doi.org/10.1002/qj.49710645013

Gaskell, W. A., Illingworth, A. J., Latham, J., & Moore, C. B. (1978). Airborne studies of electric fields and the charge and size of precipitation elements in thunderstorms. *Quarterly Journal of the Royal Meteorological Society*, *104*(440), 447–460. https://doi.org/10.1002/qj.49710444016

Gunn, R. (1947). The electrical charge on precipitation at various altitudes and its relation to thunderstorms. *Physical Review*, *71*(3), 181–186. https://doi.org/10.1103/physrev.71.181

Gunn, R. (1949). The free electrical charge on thunderstorm rain and its relation to droplet size. *Journal of Geophysical Research*, *54*(1), 57–63. https://doi.org/10.1029/jz054i001p00057

Gunn, R. (1952). The electrification of cloud droplets in non-precipitating cumulus. *Journal of Meteorology*, *9*(6), 397–402. https://doi.org/10.1175/1520-0469(1952)009<0397:teocdi>2.0.co;2

Lang, T. (2020). Remote sensing of electrification, lightning, and mesoscale/microscale processes with adaptive ground observations (RELAMPAGO) lightning mapping Array (LMA) [Dataset]. NASA Global Hydrometeorology Resource Center DAAC. https://doi.org/10.5067/RELAMPAGO/LMA/DATA101

Lang, T. J., Ávila, E. E., Blakeslee, R. J., Burchfield, J., Wingo, M., Bitzer, P. M., et al. (2020). The RELAMPAGO lightning mapping Array: Overview and initial comparison with the geostationary lightning mapper. *Journal of Atmospheric and Oceanic Technology*, *37*(8), 1457–1475. https://doi.org/10.1175/JTECH-D-20-0005.1

MacGorman, D. R., & Rust, W. D. (1998). *The electrical nature of storms* (pp. 1–422). Oxford University Press.

Macklin, W. C. (1962). The density and structure of ice formed by accretion. *Quarterly Journal of the Royal Meteorological Society*, *88*(375), 30–50. https://doi.org/10.1002/qj.49708837504

Magono, C., & Kikuchi, K. (1961). On the electric charge of relatively large natural cloud particles. *Journal of the Meteorological Society of Japan*, *39*(5), 258–268. https://doi.org/10.2151/jmsj1923.39.5_258

Medina, B. L., Carey, L. D., Lang, T. J., Bitzer, P. M., Deierling, W., & Zhu, Y. (2021). Characterizing charge structure in Central Argentina thunderstorms during RELAMPAGO utilizing a new charge layer polarity identification method. *Earth and Space Science*, *8*, e2021EA001803. https://doi.org/10.1029/2021EA001803

Mo, Q., Detwiler, A. G., Helsdon, J. H., Winn, W. P., Aulich, G., & Murray, W. C. (2007). Hydrometeor charges observed below an electrified cloud using a new instrument. *Journal of Geophysical Research,* 112(D13), D13207. https://doi.org/10.1029/2006JD007809

Nesbitt, S. W., Salio, P. V., Ávila, E., Bitzer, P., Carey, L., Chandrasekar, V., et al. (2021). A storm safari in subtropical South America: Proyecto RELAMPAGO. *Bulletin of the American Meteorological Society*, *102*(8), E1621–E1644. https://doi.org/10.1175/bams-d-20-0029.1

Pereyra, R. G., & Avila, E. E. (2002). Charge transfer measurements during single ice crystal collisions with a target growing by riming. *Journal of Geophysical Research*, *107*(D23), 4735, AAC 23-9. https://doi.org/10.1029/2001JD001279

Pereyra, R. G., Avila, E. E., Castellano, N. E., & Saunders, C. P. R. (2000). A laboratory study of graupel charging. *Journal of Geophysical Research*, *105*(D16), 20803–20812. https://doi.org/10.1029/2000JD900244

Phillips, B. B., & Kinzer, G. D. (1958). Measurements of the size and electrification of droplets in cumuliform clouds. *Journal of Meteorology*, *15*(4), 369–374. https://doi.org/10.1175/1520-0469(1958)015<0369:motsae>2.0.co;2

Reynolds, S. E., Brook, M., & Gourley, M. F. (1957). Thunderstorm charge separation. *Journal of Meteorology*, *14*(5), 426–436. https://doi.org/10.1175/1520-0469(1957)014<0426:tcs>2.0.co;2

Sartor, J. D. (1967). The role of particle interactions in the distribution of electricity in thunderstorms. *Journal of the Atmospheric Sciences*, *24*(6), 601–615. https://doi.org/10.1175/1520-0469(1967)024<0601:tropii>2.0.co;2

Saunders, C. P. R., Avila, E. E., Peck, S. L., Castellano, N. E., & Aguirre Varela, G. G. (1999). A laboratory study of the effects of rime ice accretion and heating on charge transfer during ice crystal/graupel collisions. *Atmospheric Research*, *51*(2), 99–117. https://doi.org/10.1016/s0169-8095(99)00023-x

Saunders, C. P. R., Keith, W. D., & Mitzeva, R. P. (1991). The effect of liquid water on thunderstorm charging. *Journal of Geophysical Research*, *96*(D6), 11007–11017. https://doi.org/10.1029/91jd00970

Saunders, C. P. R., Peck, S. L., Varela, G. A., Ávila, E. E., & Castellano, N. E. (2001). A laboratory study of the influence of water vapour and mixing on the charge transfer process during collisions between ice crystals and graupel. *Atmospheric Research*, *58*(3), 187–203. https://doi.org/10.1016/s0169-8095(01)00090-4

Scott, W. D., & Levin, Z. (1970). The effect of potential gradient on the charge separation during interactions of snow crystals with an ice sphere. *Journal of the Atmospheric Sciences*, *27*(3), 463–473. https://doi.org/10.1175/1520-0469(1970)027<0463:TEOPGO>2.0.CO;2

Takahashi, T. (1965). Measurement of electric charge in thundercloud by means of radiosonde. *Journal of the Meteorological Society of Japan*, *43*, 206–217.

Takahashi, T. (1972). Electric charge of cloud droplets and drizzle drops in warm clouds along the Mauna Loa-Mauna Kea saddle road of Hawaii Island. *Journal of Geophysical Research*, *77*(21), 3869–3878. https://doi.org/10.1029/jc077i021p03869

Takahashi, T. (1978). Riming electrification as a charge generation mechanism in thunderstorms. *Journal of the Atmospheric Sciences*, *35*(8), 1536–1548. https://doi.org/10.1175/1520-0469(1978)035<1536:REAACG>2.0.CO;2

Tokay, A., Wolff, D. B., & Petersen, W. A. (2014). Evaluation of the new version of the laser optical disdrometer, OTT Parsivel^2. *Journal of Atmospheric and Oceanic Technology*, *31*(6), 1276–1288. https://doi.org/10.1175/jtech-d-13-00174.1

Twomey, S. (1956). The electrification of individual cloud droplets. *Tellus*, *8*(4), 445–451. https://doi.org/10.1111/j.2153-3490.1956.tb01247.x

Webb, W. L., & Gunn, R. (1955). The net electrification of natural cloud droplets at the Earth's surface. *Journal of Meteorology*, *12*(3), 211–214. https://doi.org/10.1175/1520-0469(1955)012<0211:tneonc>2.0.co;2

Weinheimer, A. J., Dye, J. E., Breed, D. W., Spowart, M. P., Parrish, J. L., Hoglin, T. L., & Marshall, T. C. (1991). Simultaneous measurements of the charge, size, and shape of hydrometeors in an electrified cloud. *Journal of Geophysical Research*, *96*(D11), 20809–20829. https://doi.org/10.1029/91jd02262